

This article appeared in a journal published by Elsevier. The attached copy is furnished to the author for internal non-commercial research and education use, including for instruction at the authors institution and sharing with colleagues.

Other uses, including reproduction and distribution, or selling or licensing copies, or posting to personal, institutional or third party websites are prohibited.

In most cases authors are permitted to post their version of the article (e.g. in Word or Tex form) to their personal website or institutional repository. Authors requiring further information regarding Elsevier's archiving and manuscript policies are encouraged to visit:

<http://www.elsevier.com/authorsrights>



Contents lists available at ScienceDirect

Nuclear Instruments and Methods in Physics Research A

journal homepage: www.elsevier.com/locate/nima

A novel segmentation approach for implementation of MRAC in head PET/MRI employing Short-TE MRI and 2-point Dixon method in a fuzzy C-means framework



Parisa Khateri^{a,b}, Hamidreza Saligheh Rad^{a,b}, Amir Homayoun Jafari^a,
 Mohammad Reza Ay^{a,b,*}

^a Department of Medical Physics and Biomedical Engineering, Tehran University of Medical Sciences, Tehran, Iran

^b Research Center for Molecular and Cellular Imaging, Tehran University of Medical Sciences, Tehran, Iran

ARTICLE INFO

Available online 23 September 2013

Keywords:

PET/MRI

MRAC

Attenuation correction

PET

ABSTRACT

Quantitative PET image reconstruction requires an accurate map of attenuation coefficients of the tissue under investigation at 511 keV (μ -map), and in order to correct the emission data for attenuation. The use of MRI-based attenuation correction (MRAC) has recently received lots of attention in the scientific literature. One of the major difficulties facing MRAC has been observed in the areas where bone and air collide, e.g. ethmoidal sinuses in the head area. Bone is intrinsically not detectable by conventional MRI, making it difficult to distinguish air from bone. Therefore, development of more versatile MR sequences to label the bone structure, e.g. ultra-short echo-time (UTE) sequences, certainly plays a significant role in novel methodological developments. However, long acquisition time and complexity of UTE sequences limit its clinical applications. To overcome this problem, we developed a novel combination of Short-TE (ShTE) pulse sequence to detect bone signal with a 2-point Dixon technique for water–fat discrimination, along with a robust image segmentation method based on fuzzy clustering C-means (FCM) to segment the head area into four classes of air, bone, soft tissue and adipose tissue.

The imaging protocol was set on a clinical 3 T Tim Trio and also 1.5 T Avanto (Siemens Medical Solution, Erlangen, Germany) employing a triple echo time pulse sequence in the head area. The acquisition parameters were as follows: TE1/TE2/TE3 = 0.98/4.925/6.155 ms, TR = 8 ms, FA = 25 on the 3 T system, and TE1/TE2/TE3 = 1.1/2.38/4.76 ms, TR = 16 ms, FA = 18 for the 1.5 T system. The second and third echo-times belonged to the Dixon decomposition to distinguish soft and adipose tissues. To quantify accuracy, sensitivity and specificity of the bone segmentation algorithm, resulting classes of MR-based segmented bone were compared with the manual segmented one by our expert neuro-radiologist.

Results for both 3 T and 1.5 T systems show that bone segmentation applied in several slices yields average accuracy, sensitivity and specificity higher than 90%. Results indicate that FCM is an appropriate technique for tissue classification in the sinusoidal area where there is air–bone interface. Furthermore, using Dixon method, fat and brain tissues were successfully separated.

© 2013 Elsevier B.V. All rights reserved.

1. Introduction

PET is a well-known functional imaging modality because of its high sensitivity to provide molecular information, however more accurate interpretation of PET images needs to be combined with an additional anatomical imaging modality, for instance CT or MRI. Capability of MRI to provide accurate anatomical information with high soft-tissue contrast, as well as the wide range of functional information to be potentially added, has made MRI as an attractive

modality in combination with PET systems. One of the main advantages of PET imaging is its capability to provide with quantitative functional information. It should, however, be noted that the PET data is highly affected by photon attenuation in the tissues during PET data acquisition. In order to achieve accurate quantitative PET data in PET/MRI systems, it is recommended to do attenuation correction based on the MRI structural data. However, it is challenging to generate a map of attenuation coefficients using MR images, as they provide information related to proton density and relaxation properties of the tissues, but with no information about attenuation properties of the tissues. Therefore, there is no direct correlation between MR images and the μ -map at 511 keV [1].

Two main approaches to generate a μ -map at 511 keV from MR images have been proposed, including template-based methods

* Corresponding author at: Department of Medical Physics and Biomedical Engineering, Tehran University of Medical Sciences, Tehran, Iran.
 Tel.: +98 9125789765.

E-mail address: mohammadreza_ay@tums.ac.ir (M.R. Ay).

[2–4] and segmentation-based methods [1,5–7]. In the segmentation-based method, as opposed to template-based method, the relevant μ -map is directly obtained from corresponding MRI, thus there is no difficulty of abnormalities and inter-patient variations. The main focus in the segmentation-based methods is proper tissue classification in the MR images. In whole-body PET attenuation correction, it has been demonstrated that considering four tissue classes of background, lung, fat, and soft tissue provides with satisfying results [8]. In brain PET attenuation correction, it has been shown that misclassification of bone tissue leads to significant errors in PET images quantification [6]. One should note that using conventional MRI (cMRI) pulse sequences are not a suitable method for MRAC in head PET imaging because they do not provide any bone signal during the data acquisition, and therefore bone cannot be discriminated from air in the cMRI generated image. To overcome this problem, UTE techniques have been proposed to enhance the cortical bone signal, deriving appropriate attenuation map for MRAC of the head [5–7]. Nevertheless, UTE techniques are expensive as they need complicated software and hardware to be implemented; therefore they are not still widely used in clinic at least in most commercial MRI systems. As an alternative approach, ShTE sequences have been proposed by authors of this paper as more available methods [9]. Here, we suggested a combination of ShTE, 2-point Dixon (ShTEDix) pulse sequences to derive an attenuation map including cortical bone, soft tissue and air regions from MR images for the purpose of MRAC.

In this study, we focused on the development of a new MR imaging protocol in order to effectively differentiate bone from air to implement MRAC in the brain PET imaging. The proposed protocol includes ShTE pulse sequence along with 2-point Dixon method (ShTEDix) to additionally separate adipose tissue from soft tissue. It has been demonstrated that including adipose tissue in μ -map results to more precise PET attenuation correction [7]. We also concentrated on the development of image processing protocol including a modified FCM method to segment the MR images into four classes of cortical bone, soft and adipose tissues, and air regions in the head PET/MRI. The proposed procedure is now being tested statistically in a clinical study with enough number of subjects.

2. Materials and methods

The ShTEDix approach for deriving accurate μ -map at 511 keV along with optimized image processing method is described in more details as follow:

2.1. Data acquisition

Imaging protocol was development on a 3 T Tim Trio (Siemens Medical Solution, Erlangen, Germany) and on a 1.5 T Avanto (Siemens Medical Solution, Erlangen, Germany). Two normal volunteers received ShTEDix MRI scans, so that it was possible to examine each magnetic field based on one data set.

As the goal of ShTE pulse sequence is to visualize cortical bone signal before its fast decay due to its short-T2* relaxation time, the echo-time was chosen as short as possible and as follows: TE₁=0.98 ms for 3 T, and TE₁=1.13 ms for 1.5 T. To achieve highest image quality along with short echo-time, the trade-off between scan parameters was considered. For instance, there was a limitation to decrease echo-time as increasing voxel size was associated with decreasing echo-time. The repetition time of TR=8 ms for 3 T and TR=16 ms for 1.5 T were to distinction between signal intensity of eye tissue and the cortical bone, as they provide similar signals when short-echo times are used. There was also limitation to increase TR since it leads to increase total acquisition time. We also kept imaging parameters of the Dixon technique the same as the parameters of the ShTE sequence, except for the echo-times. The first echo-time of the 2-point Dixon technique (TE₂) was picked to derive an in-phase image in which water and fat signals were in-phase, and the second echo-time of the 2-point Dixon technique (TE₃) yielded an image with water and fat signal to be out-of-phase. The most important scan parameters are shown in Table 1.

2.2. Image manipulation

The acquired images from ShTE pulse sequence and 2-point Dixon method (in-phase, fat and water images) were used in order to derive a relevant μ -map of the area under imaging at 511 keV

Table 1
Scan parameters of imaging protocol for both 3 T and 1.5 T systems.

Parameters	TE1/TE2/TE3 (ms)	TR (ms)	FA	T _{scan} (min)		Voxel size (mm)	FOV (mm)
				ShTE	Dixon		
B ₀ =3 T	0.98/4.925/6.155	8	25	10	6	1 × 1 × 2	256 × 256 × 64
B ₀ =1.5 T	1.13/2.38/4.76	16	18	7.5	7.5	1.2 × 1.2 × 2	320 × 320 × 60

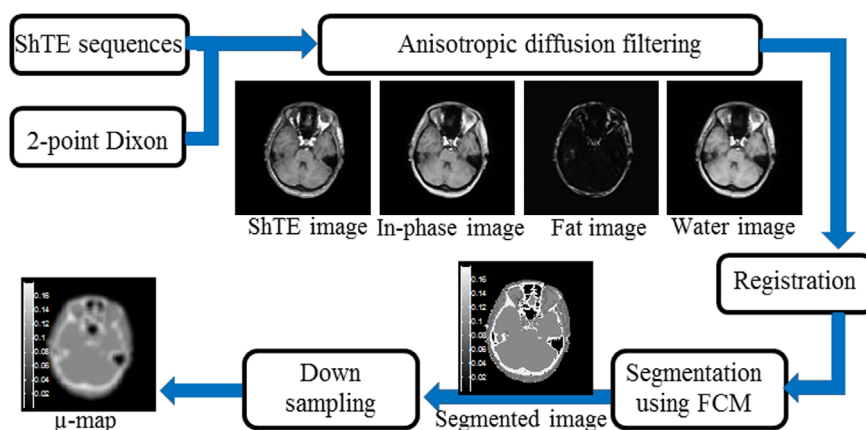


Fig. 1. The workflow of image processing algorithm.

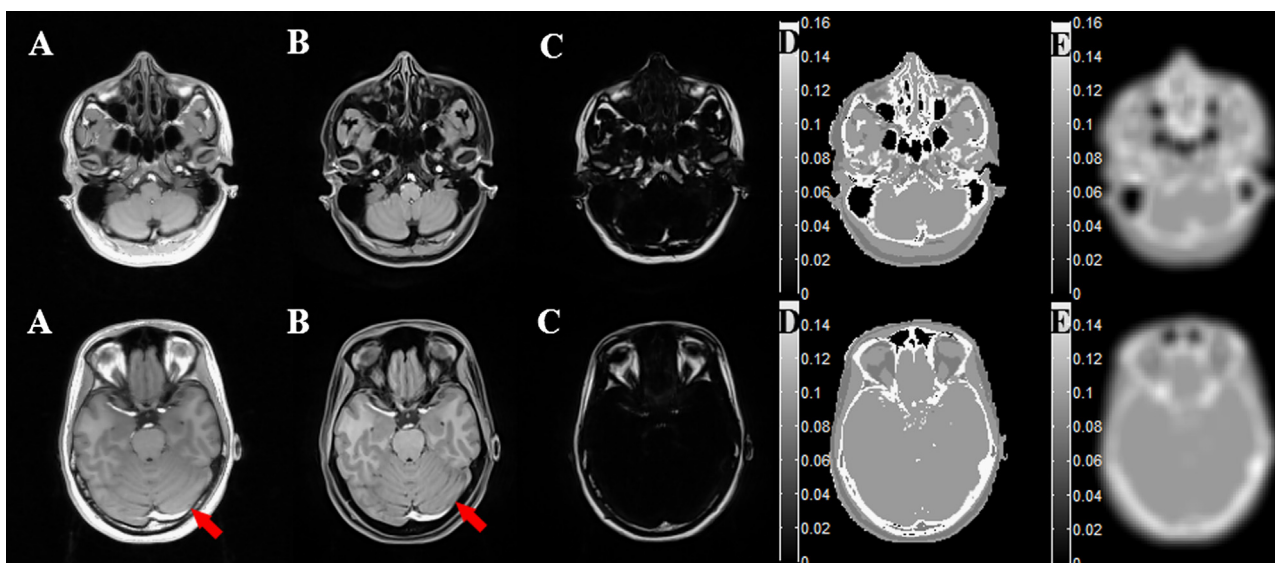


Fig. 2. ShTE images (A) from ShTE pulse sequence, water images (B) and fat images (C) from Dixon technique, segmented images of 4 classes (D) and their corresponding μ -maps at 511 keV (E) are demonstrated for 3 T MRI acquisitions. Arrows indicate cortical bone region of skull.

using segmentation-based approach. The workflow of image processing method is summarized in Fig. 1. Most of the image processing methods was implemented in MATLAB version 2010a (The MathWorks Inc., Natick, MA, USA).

2.2.1. Preprocessing

An anisotropic diffusion filtering was applied on MR images to eliminate image noise without destroying important information of the image. This filter was implemented in the open source software, 3D Slicer3 version 3.6 (<http://www.slicer.org>). After denoising, MR images were co-registered using SPM 8. The registration algorithm was based on 4th degree B-spline interpolation.

2.2.2. Segmentation

The fuzzy C-means clustering segmentation algorithm was performed on MR images, including short, in-phase, fat and water images. Fat and water masks were derived by implementing our modified fuzzy C-means algorithm on in-phase, fat and water images. The soft tissue mask (the sum of both fat and water masks) were then applied on ShTE images to differentiate bone-air regions from the soft tissue. Cortical bone and air regions were then separated by applying another fuzzy C-means algorithm on the masked short image. After the segmentation, each individual area was assigned with corresponding attenuation coefficient in 511 keV based on ICRU Report no. 44, so that cortical bone, soft tissue, adipose tissue and air regions adopted 0.173, 0.099, 0.092 and 0.000 (cm^{-1}), respectively.

2.2.3. Smoothing and down-sampling

To generate a proper μ -map, compatible with image resolution and matrix size of Discovery 690 PET/CT scanner (GE Healthcare Technologies, WI, USA), the segmented image was finally down-sampled to 128×128 matrix size and smoothed using a Gaussian filter with 6 mm full width at half maximum.

2.3. Validation

An expert radiologist manually separated bone regions, based on ShTE MR images, in 15 slices of different regions, from the bottom to the top of the field-of-view. The bone region segmented by our proposed method was then assessed based on manually

separated bone. To compare our segmentation method with the results obtained by the radiologist, the quantitative parameters of sensitivity, specificity and accuracy were calculated.

3. Results

Fig. 2 shows two slices of 3 T MRI, corresponding segmentation results and generated μ -map at 511 keV. Fig. 3 shows the same results of 1.5 T magnetic field strength. The signal intensity of the cortical bone region is shown in ShTE image compared with water image with long echo-time (arrows).

For both 3 T and 1.5 T systems, the proposed ShTEDix protocol in combination with FCM-based image segmentation yields high sensitivity, specificity and accuracy (more than 90%) for the bone segmentation algorithm. The average values for these quantitative assessment parameters were calculated on 15 slices of different regions the bottom to the top of the field-of-view of each data-set (Table 2).

4. Discussions

The proposed method in this study shows that the 4-class μ -map for the head area generated from MR data can be used for implementation of MRAC of PET data. Since there are restrictions on the use of UTE-MRI in whole-body imaging, it seems the proposed method can be a potential alternative to UTE-based PET attenuation correction in hybrid PET/MRI systems where more complex hardware is mandatory to implement UTE. This study needs to be examined in larger patient population. Furthermore, a robust validation strategy based on CT images can validate the accuracy of the proposed (ShTEDix) method.

Some area such as eye tissue and CSF were slightly misclassified as bone, while UTE-based methods also exhibit similar results. The accuracy of the algorithm for bone discrimination was higher than 90%, outside of the area of air and bone interface where susceptibility effect was observed. Exploiting the benefits to combine ShTE pulse sequence with 2-point Dixon method, MR images in the head area was segmented into four regions of cortical bone, soft tissue, adipose tissue and air.

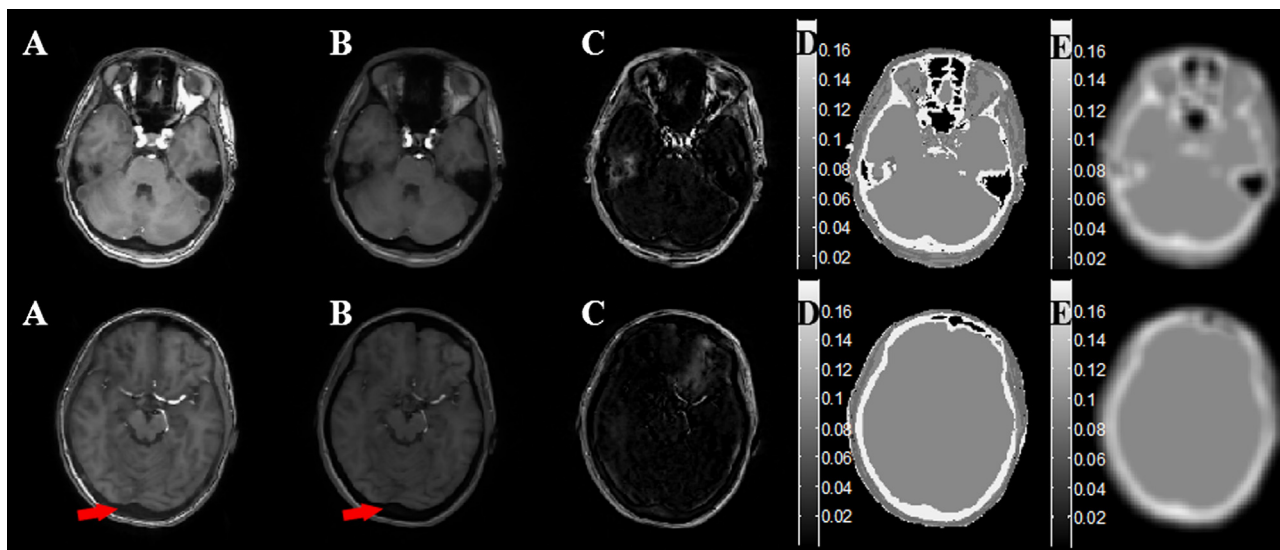


Fig. 3. ShTE images (A) from ShTE pulse sequence, water images (B) and fat images (C) from Dixon technique, segmented images of 4 classes (D) and their corresponding μ -maps at 511 keV (E) are demonstrated for 1.5 T MRI acquisitions. Arrows indicate cortical bone region of skull.

Table 2
Quantitative assessment parameters for bone segmentation (aggregated over 15 slices).

Parameters	Accuracy (mean \pm SD)	Specificity (mean \pm SD)	Sensitivity (mean \pm SD)
$B_0=3\text{ T}$	0.97 ± 0.01	0.98 ± 0.01	0.94 ± 0.02
$B_0=1.5\text{ T}$	0.98 ± 0.01	0.98 ± 0.01	0.93 ± 0.02

5. Conclusions

In this study, we developed a new approach including dedicated imaging protocol called ShTEDix and FCM-based segmentation of MR images in order to generate μ -maps for the purpose of MRAC of brain PET data. The proposed algorithm was evaluated based on few clinical data. The validation strategy in this study was based on manual segmentation by our expert neuro-radiologist. This method is still under validation requiring a large number of subjects. Furthermore, CT images should be included as gold standard.

Acknowledgments

This work was supported by Tehran University of Medical Sciences, Tehran, Iran under Grant No. 17017. The authors would

like to thank Mohsen Shojaee Moghadam and the management of Payambaran imaging centre, as well as Mostafa Robotjazi from Paitakht imaging centre and for their cooperation in the design of the MR imaging protocols.

References

- [1] H. Zaidi, M.L. Montandon, D.O. Slosman, *Medical Physics* 30 (2003) 937.
- [2] M. Hofmann, F. Steinke, V. Scheel, G. Charpiat, J. Brady, B. Schölkopf, B. Pichler, MR-based PET attenuation correction—method and validation, in: *Proceedings of the IEEE Nuclear Science Symposium and Medical Imaging Conference (2007)*, 2007, pp. 1875–1883.
- [3] I.B. Malone, R.E. Ansorge, G.B. Williams, P.J. Nestor, T.A. Carpenter, T.D. Fryer, *Journal of Nuclear Medicine* 52 (2011) 1142.
- [4] E.R. Kops, H. Herzog, Template based attenuation correction for PET in MR-PET scanners, *Nuclear Science Symposium Conference Record (2008)* 3786–3789.
- [5] V. Keereman, Y. Fierens, T. Broux, Y. De Deene, M. Lonnew, S. Vandenberghe, *Journal of Nuclear Medicine* 51 (2010) 812.
- [6] C. Catana, A. van der Kouwe, T. Benner, C.J. Michel, M. Hamm, M. Fenchel, B. Fischl, B. Rosen, M. Schmand, A.G. Sorensen, *Journal of Nuclear Medicine* 51 (2010) 1431.
- [7] Y. Berker, J. Franke, A. Salomon, M. Palmowski, H.C. Donker, Y. Temur, F. M. Mottaghy, C. Kuhl, D. Izquierdo-Garcia, Z.A. Fayad, *Journal of Nuclear Medicine* 53 (2012) 796.
- [8] A. Akbarzadeh, M. Ay, A. Ahmadian, N.R. Alam, H. Zaidi, *Annals of Nuclear Medicine* 27 (2013) 152.
- [9] P. Khateri, H.S. Rad, A. Fathi, M.R. Ay, *Nuclear Instruments and Methods in Physics Research Section A* 702 (2013) 133.